A multiscale experimental analysis of mechanical properties and deformation behaviour of sintered copper-silicon carbide composites enhanced by high-pressure torsion

Szymon Nosewicz[a*], Piotr Bazarnik[b], Melanie Clozel[c], Łukasz Kurpaska[c], Piotr Jenczyk[a], Dariusz Jarząbek[a], Marcin Chmielewski[d], Barbara Romelczyk-Baishya[b], Malgorzata Lewandowska[b], Zbigniew Pakieła[b], Yi Huang[e,f], Terence G. Langdon[f]

[a]Institute of Fundamental Technological Research, Polish Academy of Sciences, 5B Pawinskiego, 02-106 Warsaw, POLAND
[b]Warsaw University of Technology, 141 Woloska Str, 02-507 Warsaw, POLAND
[c]National Centre for Nuclear Research, 7 Soltana Str, 05-400 Otwock/Swierk, POLAND
[d]Institute of Electronic Materials Technology, 133 Wolczynska Str, Warsaw, 01-919, POLAND
[e]Department of Design and Engineering, Bournemouth University, Poole, Dorset BH12 5BB, UK
[f]Materials Research Group, University of Southampton, Southampton SO17 1BJ, UK

Corresponding author: Szymon Nosewicz (PhD), e-mail: snosew@ippt.pan.pl

Abstract

Experiments were conducted to investigate, within the framework of a multiscale approach, the mechanical enhancement, deformation and damage behavior of copper–silicon carbide composites fabricated by spark plasma sintering (SPS) and high-pressure torsion (HPT). The mechanical properties of the metal matrix composites were determined at three different length scales corresponding to the macroscopic, micro- and nanoscale. Small punch testing was employed to evaluate the strength of composites at the macroscopic scale. Detailed analysis of microstructure evolution related to SPS and HPT, sample deformation and failure of fractured specimens was conducted using scanning and transmission electron microscopy. A microstructural study revealed changes in the damage behavior for samples processed by HPT and an explanation for this behavior was provided by mechanical testing performed at the micro- and nanoscale. The strength of pure copper and the metal-ceramic interface was determined by microtensile testing and the hardness of each composite component, corresponding to the metal matrix, metal-ceramic interface, and ceramic reinforcement, was measured using nanoindentation. The results confirm the advantageous effect of large plastic deformation on the mechanical properties of Cu-SiC composites and demonstrate the impact on these separate components on the deformation and damage type.

Keywords: copper-silicon carbide composite; high-pressure torsion; metal matrix composites; multiscale analysis; nanoindentation; severe plastic deformation; small punch test.

1. INTRODUCTION

Metal matrix composites (MMCs) are an important class of materials in which the microstructure can be tailored to have superior properties by comparison with the unreinforced alloys including enhanced high-temperature performance, high specific strength and stiffness, increased wear resistance, better thermal and mechanical fatigue and creep resistance. Due to their possible applications in the aerospace, automotive, defense and general engineering industries, which require durability and long-term performance, the mechanical behavior of the MMCs is a crucial issue dominating their development.

The most significant fabrication methods, such as hot pressing [1], hot isostatic pressing [2], self-propagating high-temperature synthesis [3], pulsed and spark plasma sintering (PPS, SPS) [4-7] and arc-melting [8], are based on the use of powder metallurgy techniques. However, the fabrication of composites with extraordinary properties via powder metallurgy has several limitations including the formation of oxide layers around the metal powder particles and the clustering of particles within the material [9] so that further processing is frequently required to improve their mechanical performance. One possible alternative to applying severe plastic deformation (SPD) as the complementary technique. Thus, SPD procedures have been developed to refine the grain size in metals down to the ultrafine regime below 1 μm and thereby to enhance the mechanical strength [10-12].

High-pressure torsion (HPT) is an SPD technique incorporating the application of very high strains and it is generally considered the most efficient procedure for achieving grain refinement and strength improvement [13-17]. In this technique, a sample is subjected to high applied pressure of typically several GPa together with concurrent torsional straining. The use of a very high pressure prevents the development of cracking and segmentation even in hard-to-deform materials [18] and therefore this procedure is attractive for use in fabricating MMCs. In practice, HPT may enhance the strength of MMCs through the reduction in grain size as well as by an improved homogenization of the ceramic particles [5,9] caused by the occurrence of some or all strengthening mechanisms at a lower scale of the composite [19].

In practice, the main obstacle to the industrial application of Cu-SiC composites lies in the dissolution of silicon and carbon in the copper matrix during sintering at elevated temperatures [6, 20, 21] since this strongly influences the thermal and mechanical properties. Processing by HPT is generally conducted at room temperature and some experimental results are already available confirming the ability to use HPT for the processing of Cu–SiC composites [5,22,23]. Nevertheless, although these studies revealed an enhancement in the mechanical properties at the macroscopic level, as in increased hardness and tensile strength, these earlier results provide no quantitative evaluation of the strengthening mechanisms at the micro or nanoscale. By contrast, the multiscale analysis considers the results at different length scales and combines the efficiency of the macroscopic approach with data collected at the microscopic and nano-levels. For example, nanoindentation testing is an example of a fine-scale experimental technique that provides insight into the nanoscale mechanical behavior of each composite component [7].

The present research shows the first multiscale investigation of the mechanical properties of MMCs processed by HPT where the emphasis is placed on the improvement in the mechanical performance of the Cu-SiC composites. The effect of HPT processing on metal matrix composites has been revealed by the application of a multiscale experimental framework at the three different length scales (**macroscopic**, **microscopic**, **nano-scale)** consisting of several microstructural and mechanical testing approaches (fig. 1). The presented work focuses on the evolution of properties of composite three components – metal matrix, ceramic reinforcement and interface zone at metal-ceramic bonding area, and their impact on the composite itself. Moreover, the application of the multiscale approach allows to describe and explain the change of deformation and damage character of Cu-SiC composite subject to HPT in comparison to SPS one. The proposed framework has been presented carefully in detail in the section below.

Figure 1. The scope of the experimental multiscale framework of microstructural and mechanical characterization of copper – silicon carbide composites.

2. EXPERIMENTAL MATERIAL AND PROCEDURES

Manufacturing and microstructural characterization

Copper powder having a size of <40 μm and 99.99% purity (NewMet Koch) and SiC particles with a mean size of ~80 μm and 99.99% purity (Saint-Gobain) were used as the raw materials. Specimens containing 10 and 20 vol.% SiC particles were prepared using mechanical mixing in a planetary ball mill for 2 h with a rotational speed of 100 rpm and a ball-to-powder ratio of 5:1. The first step of material densification was the sintering of the powder mixtures using SPS within a vacuum chamber at a level of 5×10^{-5} mbar using graphite die with an internal diameter of 11 mm. To obtain well-densified materials, the sintering temperature was 950 °C with a dwell time of 10 min, a heating rate of 100 °C/min and external pressure of 50 MPa.

After the initial sintering, the samples were subjected to HPT processing. Disks with a thickness of 1 mm and diameter of 10 mm were subjected to HPT processing under an applied pressure of 6.0 GPa and rotating the lower anvil at 1 rpm through 20 revolutions at room temperature. This processing was conducted under quasi-constrained conditions which allow for a small outflow of material around the periphery of the disk during the operation.

Both initial SPS and HPT-processed samples were subjected to microstructural analysis testing. Most structural and fractography studies were conducted using scanning electron microscope (SEM) Hitachi SU-8000 operating at 10 kV and equipped with a backscatter electron detector (BSE). Detailed observations were performed using a high-resolution scanning transmission electron microscope (STEM) (Hitachi HD-2700).

Multiscale mechanical characterization

At the macroscopic scale, the mechanical properties of SPS and SPS+HPT composites samples have been determined via a small punch test (SPT). One of the main advantages of the SPT method is the fact it requires a small volume of investigated material (mostly in the shape of discs) to obtain a mechanical response. It makes SPT very useful in comparison to other mechanical tests in e.g. tensile or fracture toughness, especially in the case of HPT sample, which demonstrates the relatively small dimensions due to large plastic deformations.

The basic scheme of SPT is shown in fig. 2. In the presented work the testing was performed at a universal Zwick/Roell Z005 testing machine with a 5 kN load cell and a punch displacement rate of 2.0 mm/min. An electromechanical extensometer MTS 634-12F-25 was applied for measurements of the material deflection using disk-shaped specimens with diameters of 8 mm and heights of 0.6 mm. The SPT samples were cut off from the middle of the HPT disc. For each material state, 3-5 discs were investigated. The testing temperature was 25°C (marked as RT) and 350°C measured by a thermocouple located in the testing stand. For higher temperatures, the samples were held 10 mins at the designed temperature before SPT. The samples were mounted between two dies, which were further immobilized by a screw. The nut was screwed to a sleeve, with 15 Nm torque. For sample deformation, a spherical punch of 1 mm radius was used and the results of SPT were recorded as force-displacement curves for the punch. The ultimate force (Fu) was recorded as the maximum registered force.

The application of a biaxial state of tension by bending the miniature disk-shaped specimens causes a complex stress condition usually making impossible recalculation of stress and strain directly from the register data. However, since the dimensions of samples are presented, we found it valuable to use SPT in the proposed work (similarly as [24,25]) for the comparison between two states of materials (SPS and SPS+HPT) using force and deflection curves and in that way show the impact of HPT on macroscopic composite properties.

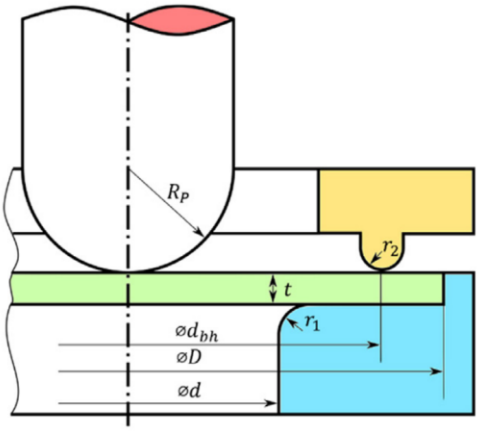

Geometrical parameters

Punch radius	$R = 1$ mm
Specimen diameter	$D = 8$ mm
Specimen thickness	$t = 0.8$ mm
Inner bottom die diameter	$d = 5.4$ mm
Specimen holder diameter	$d_{bh} = 6.2$ mm
Die chamfer radius	$r_1 = 0.4$ mm
Specimen holder radius	$r_2 = 0.4$ mm

Figure 2. Principle sketch of the experimental setup of small punch test [6].

At **the microscopic scale**, the microtensile strength test of pure copper and the interfacial copper-silicon carbide bonding test has been performed. The microscopic tests were conducted via the procedure presented in [26]. The sample radius was 2 mm with a reduced section of around 1 mm. Sandpaper was used to further decrease the sample thickness and a chemical selective Cu etching was used for final finishing. The composition of the etchant was: acetic acid ($C_2H_4O_2$, 10 ml), hydrogen peroxide (H_2O_2, 10 ml), and distilled water (H_2O, 80 ml). An example of a sample of Cu-SiC composite material in the form of a beam is shown in fig. 3. Samples were carefully mounted in tensile tester by means of epoxy resin to avoid standard mechanical squeezing (fig. 3a) and etchant was applied precisely by pipette and was used to reveal a Cu-SiC interface and also to avoid destroying soft and thin sample while mounting (fig. 3b). The displacement was forced by a stepper motor and the force was measured using a strain gauge force sensor. The velocity of displacement was set 0.01 mm/s. The ultimate tensile strength is defined as the force which breaks the rod at the interface, divided by the area of the interface:

Commented [M1]:

$$\sigma = F_a / S \quad (1)$$

where F_a is the adhesion force between the metal matrix and a particle and S is the projected contact area. To determine the contact area, an optical microscope was used.

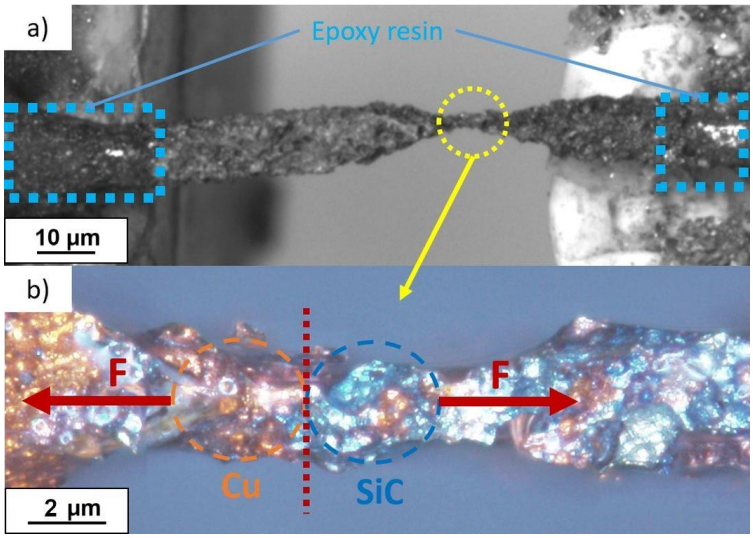

Figure 3. Cu-10%SiC composite manufactured by HPT a) general overview by digital camera b) Cu-SiC interface by optical microscope.

At the nanoscale, hardness, plastic and maximum depth were measured by using the nanoindentation technique. Studies were performed on a NanoTest Vantage® system developed by MicroMaterials Laboratory MML. All the experiments were conducted by using a Berkovich-

shaped diamond indenter. Before indenting each specimen series, the equipment was calibrated and the diamond area function (DAF) of the indenter tip was determined. A calibration procedure was completed by performing a series of indentations with a maximum load of 1 mN. As a test matrix with known properties, fused silica was used. The performed DAF calculations were in line with the ISO 14577 standard. Afterward, the calculated DAF was used at every stage of the analysis of the results. A thermal measurement period of 60 s was performed at the end of each indentation, the results of which are used to correct the indentation data during analysis. Several indentation techniques were employed:

- Targeted indentations: An area of 100 x 100 µm is scanned using the Berkovich indenter with a piezostage, providing a map of the surface (see fig. 4) by moving over the surface and using a very low force (0,002 mN). However, because the imaging procedure is based on the mechanical contact of the sample and the indenter, and because the step size is 0,5 µm, the image resolution is lower than a typical AFM image. 12 to 15 indents using a maximum load of 1 mN, with 10s loading, 5s holding, 5s unloading times are then performed in locations chosen after the mapping. The goal of this procedure was to indent intentionally: (i) metallic substrate, (ii) ceramic particles and (iii) interface-like region.
- Mappings: 10x10 indents were performed using a maximum load of 1 mN, with the following times: loading 10s, holding 5s, unloading 5s, leaving 100 µm between indents to avoid with certainty any interaction between indents. Reported procedure allowed one to cover 1 mm^2 of the surface and determine hardness profile over probed surface area.

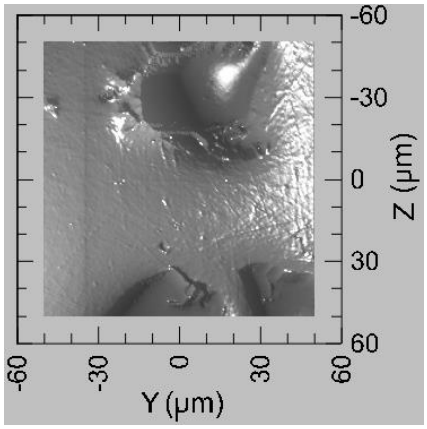

Figure 4. Example of the surface scan obtained by piezo-stage stage option.

After the indentations, all load-unload curves were fitted by using the Oliver-Pharr method [27]. The goal of such detail analysis, involving conducting measurements in three volume scales was to perform a comprehensive structural and mechanical analysis of the studied system, obtain time and scale independent data which will help us to better understand occurring phenomena.

3. EXPERIMENTAL RESULTS

3.1. Microstructural characterization after HPT processing

Processing by HPT leads to a significant change in the pure copper and copper-silicon carbide composites. Based on microstructure analyses of SPS-processed samples performed earlier [20, 21], the copper and copper-silicon carbide samples show grain inhomogeneity due mainly to the non-uniform rate of grain growth and recrystallization processes (fig. 5a). The microstructure of the SPS samples also revealed a high fraction of nano- and micropores in the copper matrix. The presence of residual porosity was confirmed by density measurements which gave a relative density of the Cu-SiC composite fabricated by SPS at ~98% [21]. These microstructural characteristics may affect the material strength in an undesirable way but it appears that their influence is minimized by the use of HPT processing. Due to the application of significant compressive and shear stresses during the plastic deformation, practically no pores or voids were visible in the metal matrix (fig. 5b). This effect is confirmed by density measurements for the Cu-10% SiC and Cu-20% SiC composites processed by HPT where the measured values were ~99.5% ± 0.2 %. Furthermore, the average copper grain size after HPT processing was ~350 nm which is significantly smaller than for the SPS sample [5].

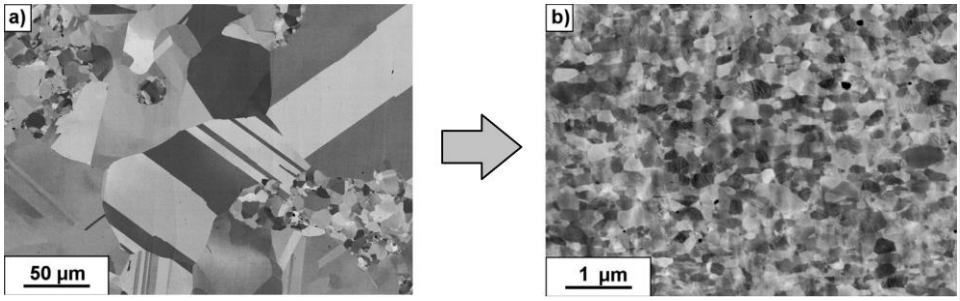

Figure 5. Evolution of pure copper microstructure after SPS (a) and subjected to the HPT process (b).

On the other hand, the impact of large stresses during HPT was not sufficient to fully fragment the largest SiC particles and these are visible in the samples where they tend to display numerous internal cracks and discontinuities (fig. 6). In practice, many of the large ceramic particles become fragmented into smaller particles thereby creating agglomerates that reduce the overall strength of the system. Moreover, due to their low fracture toughness, most of the ceramic SiC particles evolve into clusters of particles having sizes between ~0.05 and ~6.0 µm. The microstructure also displays a high fraction of fine SiC particles with sizes of ~50 – 700 nm, which are dispersed and reasonably homogeneously distributed within the copper matrix. Significant changes of metal matrix and ceramic reinforcement structure should be reflected in the mechanical behavior of the material at three investigated scales.

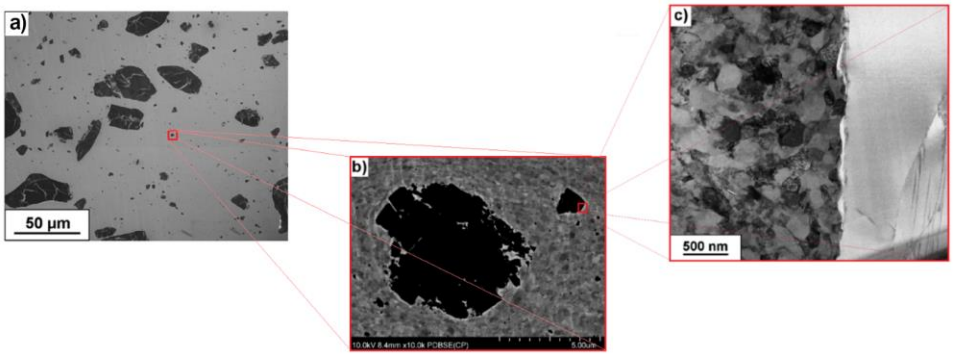

Figure 6. The microstructure of Cu-20%SiC composite after HPT process (a, b) with additional TEM images (c).

3.2. Mechanical properties at the *macroscopic* scale

Revealed microstructure evolution after HPT processing should be reflected in the adequate evolution of material's mechanical properties at the macroscopic scale. Here, the mechanical properties were evaluated by small punch tests on pure copper and copper matrix composites with 10 and 20% vol. content of silicon carbide samples fabricated by SPS and SPS+HPT. Representative force-deflection (F-D) curves of Cu and Cu-20%SiC samples registered during the SPT test in RT and 350ºC have been shown in fig. 7. Based on F-D curves, the ultimate force has been evaluated and presented in fig. 8.

It is readily apparent that the F_u was higher for all specimens after plastic deformation processing by HPT, where the increases were of the order of 64-70% for both Cu-SiC composites tested at RT and 350ºC, but it was associated with a loss of plasticity, measured by specimen deflection to failure. Loss of plasticity of SPS+HPT samples is especially evident in the case of composites, which indicates even five-six times lower deflection in respect to SPS one. In the case of pure copper, this effect is much lower both at RT and at a higher temperature. Furthermore, it is seen the impact of applied temperature during tests on material's mechanical properties. Similar to the case reported in [6], it was shown the unfavourable influence of temperature on pure copper and composite strength during small punch testing. On the other hand, even though all materials deformed at 350°C revealed smaller ultimate force, they show a higher deflection to failure in comparison to RT. Finally, the effect of the SiC reinforcement on the copper matrix was studied for both the SPS and HPT specimens and, as expected, for SPT the highest maximum force was obtained for pure copper at both studied temperatures.

The evolution of material's mechanical properties is accompanied by the shift of damage mode. Figure 9 shows the representative images of fracture surfaces of the samples after macroscopic strength tests. Both copper samples fabricated by SPS and SPS+HPT (figs 9a and b) exhibit ductile character with evidence for dimples, micro-voids and necking in macro observations. It is worth noticing, mentioned features are more apparent in the SPS sample case.

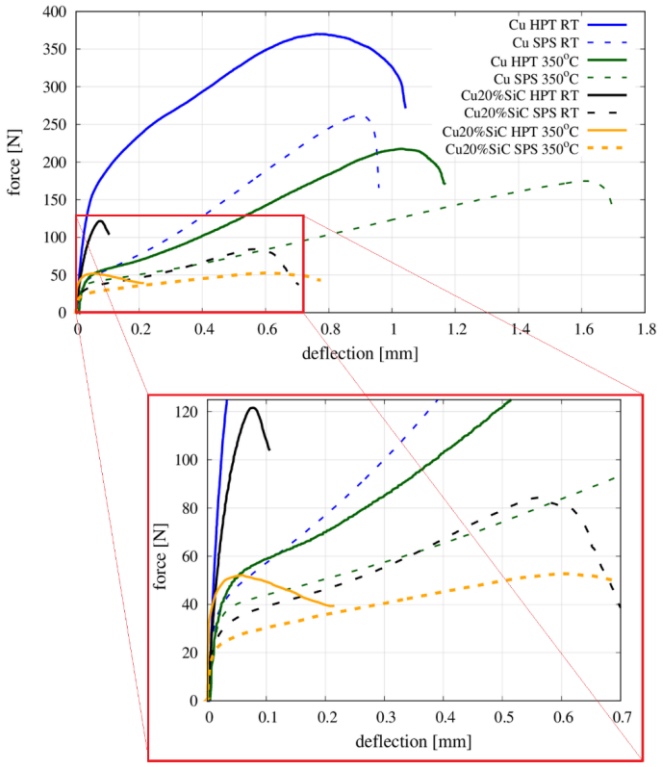

Figure 7. Representative force-deflection curves of pure copper and Cu-20%SiC composite processed by SPS and SPS+HPT registered during SPT test in RT and 350ºC.

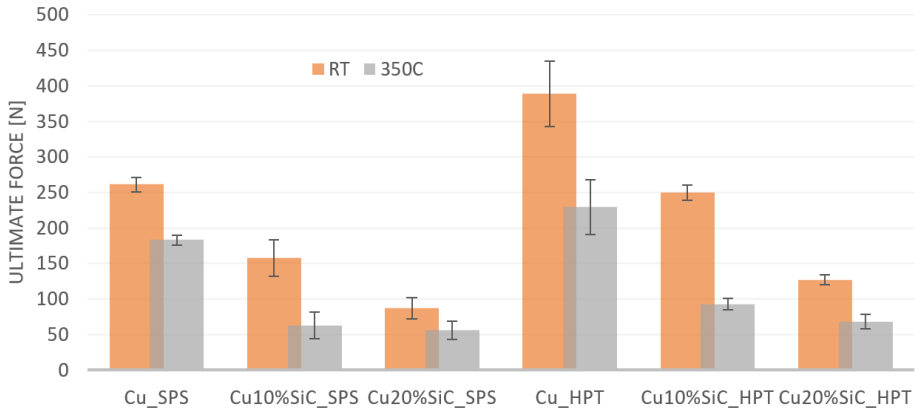

Figure 8. The ultimate force results of the small punch test performed at the macroscopic scale.

The SPS Cu-10% SiC and Cu-20% SiC samples displayed similar fracture surfaces as shown in figs. 9c and e. Cracks were initiated at micro-voids and discontinuities occurring at the interfaces between the SiC particles and the Cu matrix and propagated intergranular along with the weak bonding without damaging the particles. Conversely, SPS+HPT composite samples fracture indicates the combination of trans- and intergranular damage as shown in figs. 9d and f. On the one hand, it can be seen the ductile fracture within the Cu matrix with additional cleavage fracture of the SiC particles, and on the other hand, the pulled out the ceramic reinforcement from the metal matrix pointing to intergranular damage along the interface zone.

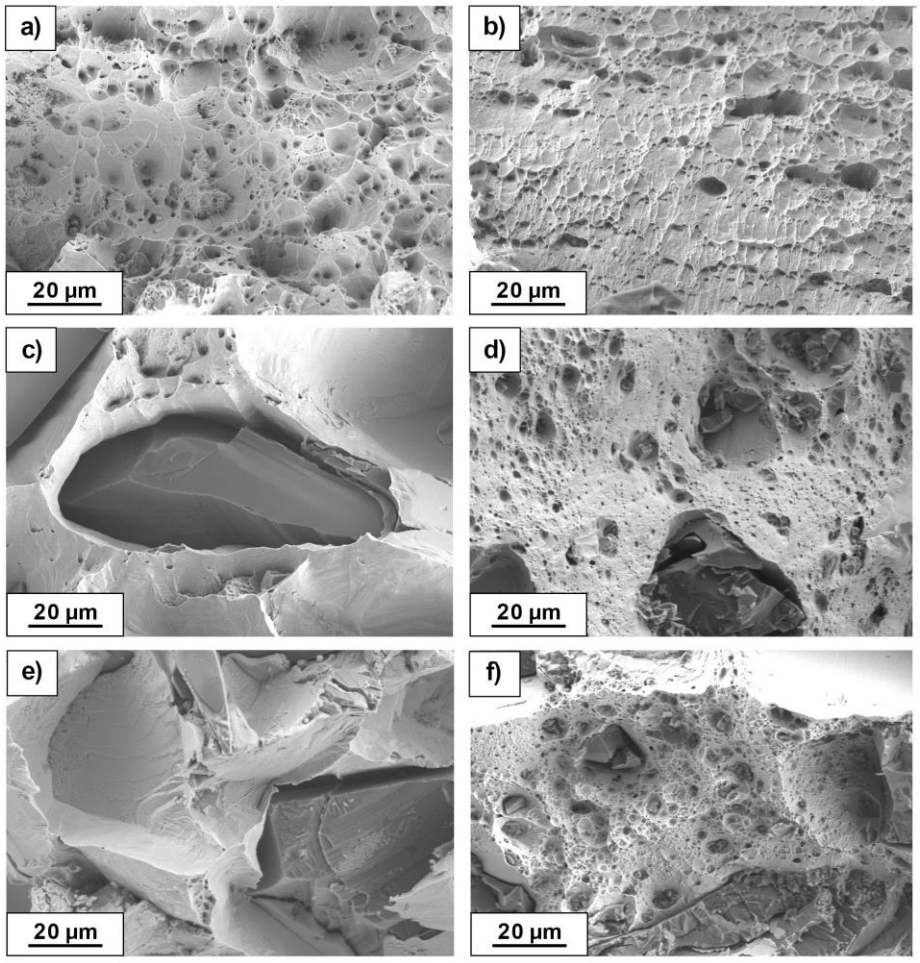

Figure 9. The representative images of the fracture surface after **test: a) Cu SPS, b) Cu HPT, c) Cu-10%SiC SPS, d) Cu-10%SiC HPT, e) Cu-20%SiC SPS, f) Cu-20%SiC HPT.**

3.3. Mechanical properties at the *microscopic* scale

The main aim of microscopic experiments is to qualitatively determine the tensile properties of the pure copper and the interface between matrix and ceramic SiC reinforcement in the context of mechanical improvement of each composite component after HPT. The tensile experiments with very careful sample preparation have been performed using the procedure presented in Sec. 2.

Since the velocity of the holder and the cross-sectional area of the broken bonding are known, it was then possible to determine the engineering stress-displacement curves. It would also be interesting to evaluate strain, however the estimation of the initial length or the length of the reduced section is hindered). Nevertheless, representative curves of the tensile testing are shown in figs. 10a and b for pure copper and Cu-10% SiC in the initial state and after HPT processing. The results of pure copper bonding fabricated by SPS brought a weaker response than SPS+HPT. Furthermore, pure SPS copper exhibited significant plastic deformation whereas HPT copper was more brittle with a dominant elastic range. In the case of interfacial bonding tensile strength test of copper and silicon carbide particles, both SPS and SPS+HPT samples indicate a pure elastic and brittle character in the full range of deformation. The samples broke in a brittle manner, however for the second one, the change in a curve slope is visible. We tentatively attribute it to the change in the resultant sample stiffness due to the delamination of interfaces other than studied particles. It is worth mentioning that during epoxy resin solidification tensile force increased from 0 to 4 N (about 8% of max. tensile force). To minimize such an effect one should move a holder to obtain force equal to 0 N a couple of times during solidification. As the time and velocity of the holder are known, it is possible to determine displacement and knowing the area of the initial cross-section one can calculate engineering stress so force-time and engineering stress-displacement curves are of the same shape. Figures 11a and b present the fracture surfaces of a broken Cu-SiC SPS sample, ceramic reinforcement side and copper side, respectively.

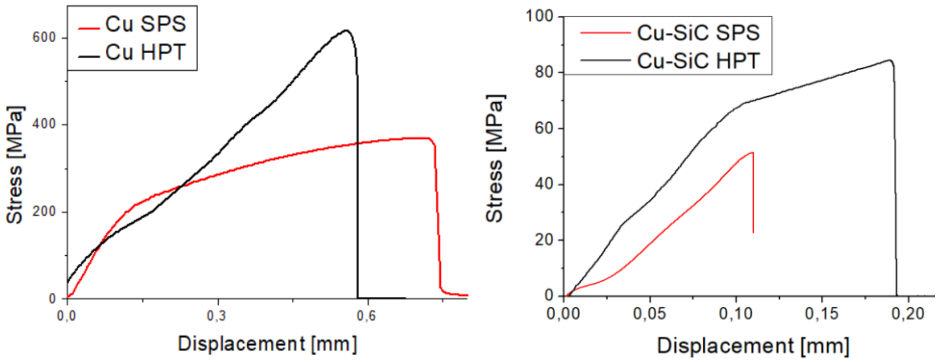

a) b)

Figure 10. Engineering stress- displacement curves of microtensile testing for a) pure Cu-Cu, and b) Cu-SiC bonding.

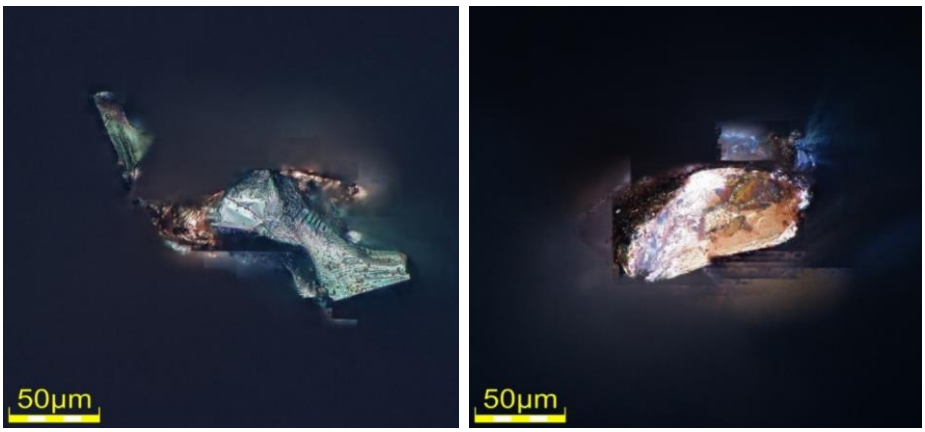

a) b)

Figure 11. Optical microscope images of a rod consisting of the Cu and SiC particles subjected to tensile testing: a) silicon carbide side and b) copper side after the experiment.

The values of the ultimate tensile strength UTS, shown in Table 1, demonstrate significant material enhancement after the HPT processing for both pure Cu and Cu-SiC bonding. The ultimate tensile strength of pure copper increases from 370 to 529 MPa. The mechanical enhancement of Cu-SiC bonding is not such spectacular as in the Cu matrix, however the rise of UTS by around 40% is also a considerable result.

Table 1. Results of microtensile strength measurements.

	Pure Cu SPS	Pure Cu HPT	Cu-SiC SPS	Cu-SiC HPT
ultimate tensile strength [MPa] with standard deviation	**370**± 100	**529** ± 87	**54** ± 5	**85**±5

The microtensile testing allows to reveal the advantageous impact of HPT on the micromechanical component of the composites, however it should be mentioned about several unfavorable aspects of the microtests. Uncertainty of measurements can be caused by a couple of factors: the rapture of the sample takes place not necessarily in the thinnest cross-section and also could occur in the plane non-perpendicular to a direction of tensile force, mounting samples with epoxy resin does not provide precise control of collinearity of sample axis and tensile force direction, machining of the samples could interfere in internal stresses. Moreover, the real contact area is estimated as the area of cross-section before the tensile test. Values of uncertainty are calculated as expanded uncertainty of combined standard uncertainty which takes into account the factors mentioned above.

3.4. Mechanical properties at the *nanoscale*

The nanomechanical properties of the ceramic phase, the metallic matrix and their interface region were measured by nanoindentation using two procedures: targeted indentation and mapping. Targeted indentations were performed to collect data from all three phases and fig. 12 displays examples of the Cu-SiC composite regions, with sizes of 100 × 100 μm^2, with dots indicating the positions of the nanoindentations. In order to differentiate between the phases, individual colors are assigned with black for the ceramic, red for the metal and blue for the interface region: these colors are used in figs. 12-14. It should be noted that the images presented in fig. 12 relate to the mechanical contact of the indenter tip with the sample surface using the so-called reverse AFM procedure [7].

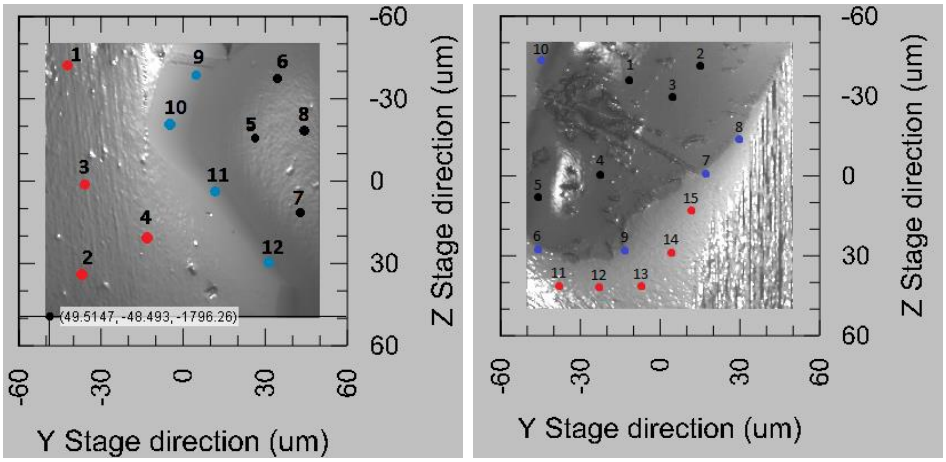

a) b)

Figure 12. Surface scan performed using piezostage option and recorded on a metallic substrate (red dots), ceramic particle (black dots) and interface-like region (blue dots) L-D nanoindentation curves (see fig. 15) in: a) Cu – 20%SiC SPS and b) Cu – 20%SiC HPT samples.

The nanoindentation load-depth curves in fig. 13 are the result of targeted indentations without any data smoothing. All nanoindentations used a load of 1 mN which corresponds to a penetration depth of ~20–160 nm depending on the phase. Relatively small loads were used to accurately compare different regions of the composite by probing small volumes. Since the SiC is a hard material embedded in a soft Cu substrate, the application of a high load may result in the rotation of the SiC into the softer Cu. Therefore, to obtain an accurate estimate at the nanoscale, each phase was tested at least four times and the average values are given in Table 2.

Commented [M2]: Dlaczego rotation?

Table 2. Hardness, plastic and maximum depth recorded during nanoindentation test of individual phases: Cu – copper metallic matrix, I – interface region and SiC – ceramic silicon carbide reinforcement.

Material	Hardness (GPa)			Plastic depth (nm)			Maximum depth (nm)		
	Cu	*I*	*SiC*	*Cu*	*I*	*SiC*	*Cu*	*I*	*SiC*
Cu SPS	1.1	-	-	150	-	-	156	-	-
Cu HPT	1.5	-	-	125	-	-	132	-	-
Cu-10%SiC SPS	1	17	31	154	60	12	160	68	21
Cu-10%SiC HPT	1.6	2.7	20	118	100	18	124	108	28
Cu-20%SiC SPS	1.2	19	31	138	34	12	144	42	21
Cu-20%SiC HPT	1.6	3.3	25	117	90	15	123	97	24

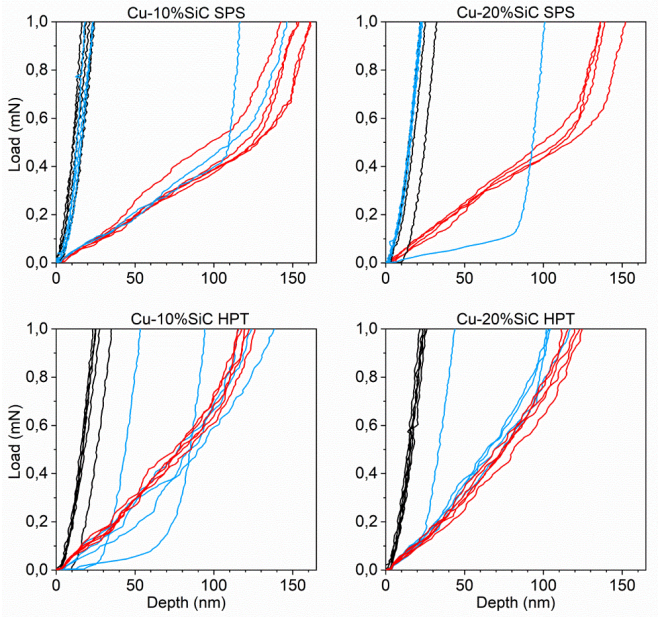

Figure 13. Individual load-displacement curves obtained from targeted indentations.

The authors would like to point out that the interface results, in this case, are only given as additional information showing the general tendency of material/phase evolution for the following reasons. Firstly, as schematically shown in fig. 14, depending on the orientation and position of the SiC carbide below the surface, the interface zone may not prolong directly beneath the indent. Indeed, the carbide may find itself a short distance beneath the indent (case "interface 1"), or be further from the indent position as the depth increases (case "interface 2").

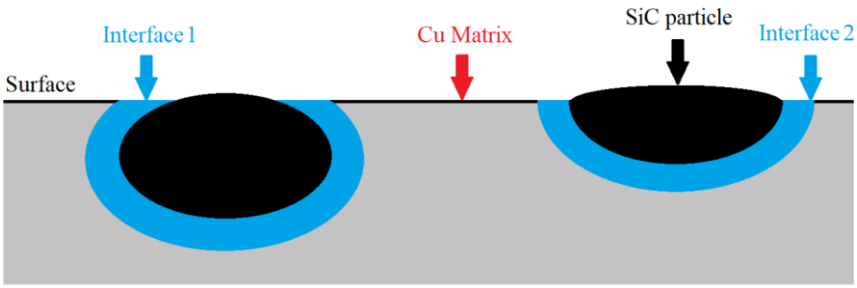

Figure 14. Schematic representation of a cross-section of the bulk of Cu-SiC, near the surface, along with examples of indentation points.

Although in both cases, the indents would be placed at similar distances from the boundary of the carbide as seen from the surface, they would yield considerably different results. Indeed, the indenter probes a volume extending approximately even 10 times the indentation depth along the general direction of application of the force, and perpendicular to that force approximately 6 times the indentation radius near the surface, forming a half-ellipse. This means that invisible objects below the surface will affect the mechanical properties evaluated from the load-displacement curves. Secondly, the resolution of the image obtained for targeted indentation is not as good as with AFM, for example. In fig. 12 a), the borders of the carbide are not obvious, hence when choosing indentation coordinates, one cannot be sure whether one is indeed indenting close to the carbide, or directly above it. Thirdly, because of the large difference in mechanical properties between matrix and carbides, the carbides tend to protrude after polishing, making the surface uneven and causing the automatic surface detection at the interface to sometimes be inaccurate. Lastly, the indents may not be performed exactly where the coordinates are placed, which is relevant in the case of indentation of the precise and narrow interface zone. Because of these reasons, the load-displacement curves in fig. 13 obtained from targeted indentations of interface areas are not perfectly uniform, however, on the other hand, they should not be significantly burdened with the abovementioned effect. Despite these controversies, the nanoindentation technique is currently the only method that allows probing small volumes of the materials. Since the goal of this work is to understand and explain the mechanical behavior of a very challenging system like Cu-SiC, we took an effort and despite some procedural pitfalls we intend to critically assess obtained nanomechanical data, as this may have critical importance in the further development of this material.

Following the targeted indentation, mapping experiments were performed. The results of these tests are presented in figs. 15 and 16. The presence of carbides can be easily distinguished from the matrix in both figures, as they are characterized by much higher H values. As mentioned previously, the indenter probes volume of the material which extends further than the indent itself. In our investigation, the information is collected from the volume extending approx. 1,5 µm in depth in the case of Cu SPS, and approx. 1,3 µm in the case of Cu HPT.

The nanoindentations show that the copper produced by HPT has a higher hardness than that produced by SPS, however, this hardness could be overestimated due to different plastic behaviors: under micro-indentation (with loads up to 5 N, i.e. 5000 times greater than with nanoindentation), Cu HPT forms more pile-up around the indenter than Cu SPS, leading the device to underestimate the indentation depth, hence, leading to overestimation of the hardness. Further analysis would be required to verify whether this is also the case with the loads employed during nanoindentation (using AFM, or analysis of indent cross-sections in SEM, for example).

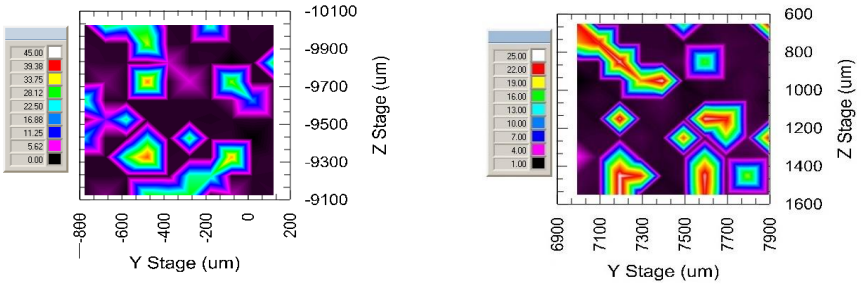

a) b)

Figure 15. Mapping of hardness results for: a) Cu – 20%SiC SPS and b) Cu – 20%SiC HPT samples. Hardness values in GPa.

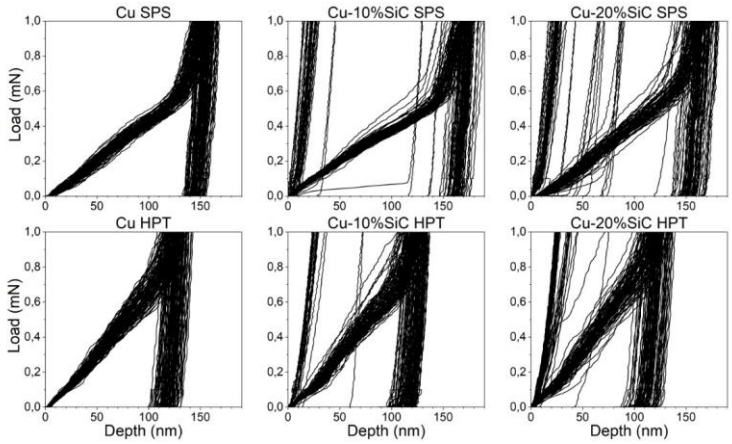

Figure 16. Load-displacement curves obtained from mapping tests.

4. DISCUSSION

Generally, one main conclusion can be made from presented mechanical tests performed on three separate scales. As was expected, the high-pressure torsion has affected significantly both pure copper and copper-silicon carbide composites. Explanation of such enhancement of metal matrix composite has its origin in the strengthening effects of the material across the scales at each composite component: metal matrix, ceramic reinforcement and metal-ceramic interface.

4.1. The impact of HPT processing on the metal matrix

The application of HPT refers to substantial improvement in the copper mechanical properties. In practice, obtained grain refinement and elimination of residual porosity (fig. 5) result in the increase of the strength and hardness through the Hall-Petch relationship but there is also a slight reduction in the elongations to failure as determined in microtensile tests (fig. 10). This effect is also observed at the nanoscale in fig. 13. Nanoindentation tests show an increase in hardness and a decrease in plastic depth in the copper matrix after HPT as documented in Table 2. This effect is also visible in the various load-displacement curves obtained from targeted indentations which differ depending on the processing method as shown in fig. 13. Thus, the curves of the Cu matrix from the SPS samples in figs. 13a and b display a relatively substantial elastic range and subsequently the plastic one, while those after HPT are steeper without a clear plastic zone [29].

The nanoindentation study offers another conclusion related to the SPS+HPT materials. Specifically, the presence of SiC particles leads to an increase in hardness of the copper matrix compared to pure copper. As was confirmed earlier at the microscale during micro indentation tests [5], the hard and tightly packed SiC particles obstruct the movement of dislocations.

Presented results are generally consistent with the behavior of ultrafine-grained and/or nanocrystalline FCC materials [30]. The main feature of these materials, including SPS+HPT copper and copper matrix composite, refers to an induced large number of various types of defects: a high density of dislocations, the significant volume fraction of grain boundaries and small vacancy clusters forming by agglomeration of deformation-induced vacancies [31]. As a result, the favorable combination of high strength and satisfied ductility can be preserved [32].

4.2. The impact of HPT processing on the ceramic reinforcement

The mechanical and microstructural properties of silicon carbide particles change dramatically due to the application of HPT processing. Several reasons explain such a transition. Generally, the particles in SPS samples retain their initial dimensions within the range of ~10 to ~100 μm despite the mixing process, which has little or no effect on the ceramic particle size [6]. The bonding between the silicon carbide reinforcement particles does not display a cohesive/diffusive character because of the limited sintering processing conditions. Consequently, small amounts of microporosity are produced between the ceramic particles and this is a potential source for crack initiation where the HPT processing improves the homogenization of the composite microstructure

and produces a more uniform distribution of SiC particles. For the HPT Cu-20% SiC samples, this leads to significant refinement of ceramic particles (figs. 6, 9d and 9f).

Ceramic nanoparticles, obtained as a result of HPT processing, create an advantageous system with reference to the macroscopic composite strength and they provide a high mechanical resistance due to several strengthening mechanisms such as the Orowan effect or the load-bearing effect or load transfer between the matrix and the reinforcement [33-35]. This reinforcing mechanism is effective only if a strong cohesion is achieved between the matrix and the reinforcement [36].

A well-defined dual impact of HPT processing on the mechanical properties is evident in the nanoindentation investigation. Firstly, there is a weakening of SiC after HPT with respect to SPS for all compositions. The weakening resulting in the lower hardness of the ceramic phase of the HPT samples is attributed more to the cracking and damage of the SiC particles after application of sizable forces during processing than the plastic deformation resistance. In contrast to the ceramic particles after HPT, the solid and undamaged SiC reinforcement after SPS shows higher resistance to the applied load during nanoindentation testing.

Secondly, after HPT the SiC particles exhibit higher hardness levels as the ceramic content rises. Thus, applying HPT to Cu-20% SiC composites leads to more effective fragmentation and in this way it lowers the numbers of relatively large SiC particles while simultaneously increasing the numbers of nanoparticles which benefits the mechanical properties at the nanoscale.

4.3. The impact of HPT processing on the metal-ceramic interface

The presence of SiC particles increases the hardness of the copper matrix due to the Orowan strengthening mechanism but, at the macroscopic scale, the Cu-SiC composites fabricated by SPS and HPT both exhibit lower strengths compared to pure copper (figs. 7 and 8). In practice, the addition of ceramic particles to the metallic matrix leads to an increase in the number of metal-ceramic interfaces and these are the weakest links when measuring the material strength [6]. These interfaces are defined as two-dimensional zones wherein one or more material parameter exhibits a discontinuity [37] and this has a significant impact on the macroscopic properties such as the yield strength, fracture behavior, thermal expansion and/or conductivity [38-40]. The importance of the interface may be examined in terms of two general aspects. Firstly, the physical state of the interface and the presence of material defects that may change the properties at or near the interface itself. Secondly, the chemical state of the interface since a new phase may form during processing due to interactions between the metal matrix and the ceramic reinforcements.

These effects are found in copper-silicon carbide composites processed by SPS in which the physical structure of the Cu-SiC interface reveals a high fraction of nano- and micropores. Furthermore, new phases may be formed in the matrix-reinforcement bonding region which will influence the mechanical properties [6,7,20,21]. In the area of the interface zone, silicon carbide decomposes to silicon and carbon in contact with copper and the silicon dissolves into the copper matrix to form a Cu_3Si phase with a residual carbon layer [21, 41-44].

In practice, the microstructural features of the Cu-SiC interface zones of samples prepared by SPS contribute to the mechanical response. Assuming that the composite strength at the

macroscopic level is mostly affected by the metal-ceramic interface, experimental results obtained at the microscopic level should assist in interpreting the data. However, there is no evidence for any voids, debonding or cracking in the contact zones between the copper matrix and the SiC reinforcements after HPT (fig. 6). Processing also improves the adhesion between the soft matrix and the hard particles through an enhanced dislocation density strengthening mechanism [45]. The metal-ceramic interfaces become areas of residual plastic strain and this increases the dislocation density due to the matrix/reinforcement elastic modulus mismatch and work hardening during the deformation process [46]. Additionally, the high compressive and shear stresses lead to large microstructure transitions within the Cu-SiC contact zones, leading to the annihilation of Cu_3Si and the residual carbon layers. This means that the SPS+HPT-processed Cu-SiC composites indicate higher strength of interfacial metal-ceramic bonding than after SPS processing as shown in Table 1.

Using nanoindentation as summarized in Table 2, the hardness of the interfaces in both the 10% and 20% SiC SPS samples is higher than for the HPT samples. This is attributed to the development of an interfacial Cu_3Si phase and residual carbon. The presence of new phases/layers in the metal-ceramic interface zone may lead to an increased material volume response during indentation and a carbon structure will combine relatively high strength with a brittle character of deformation to therefore display higher resistance to compressive loading. Since the interfacial zone in the HPT samples lacks any additional phases/layers, it gives a lower response than in the SPS samples. An additional phenomenon is presented in fig. 14 where the larger SiC particles in the SPS samples increase the possibility of indentation at their surface rather than indenting the interfacial zone. Conversely, the HPT interface consists of both large and fine SiC particles so that the possibility of SiC indentation is smaller and the recorded nanohardness values may represent the true mechanical properties of the interfaces.

Both the SPS and HPT interfaces reveal higher hardness values as the SiC content increases. This effect is due to an enhanced dislocation density due to the thermal inconsistency between the copper matrix and the silicon carbide. During the cooling process, thermal stresses around the reinforcement are sufficiently large to generate plastic deformation in the matrix and this is especially anticipated in the contact bonding region [47]. These stresses induce dislocations within the area of the matrix-particles interface [48-50] which may accumulate with increasing reinforcement content. For the HPT interface, this effect is stronger due to the copper grain refinement and fragmentation process of the ceramic phase during processing, resulting in the formation of a more highly developed nanostructured microstructure. This will lead to a strengthening of the interface zone which is also responsible for the higher hardness of the metal-ceramic interface in both the SPS and HPT composites compared to the copper matrix.

4.4. The impact of HPT processing on the deformation and damage behavior of the overall system

Evaluation of deformation and damage behavior can be made from the investigation of force-deflection curves from small punch testing. Apart from the fact, they bring quantitative data from

the test, such as an ultimate (maximum) force or maximum registered deflection, they allow qualitatively assess the behaviour of the material. The shape of the F-D curve can be an important indicator confirming if material breaks in a ductile, brittle, or mixed manner. Similar analyses have been carried out in several works regarding the numerical and experimental investigation of SPT [24,25]. Knowing the F-D curves for typical ductile and brittle material, we can assign studied SPS and SPS+HPT materials to each type of deformation and damage. To facilitate the determination of the F-D curve shape and its features, it was introduced the parameter $\dot{F}$ related to curve slope and defined as the first derivative of registered force with respect of deflection - $\dot{F} = \mathrm{d}F/\mathrm{d}u$. Having this parameter normalized by its maximum value - $\dot{F}/\dot{F}^{\max}$, it is possible to catch any change of slope indicating the deformation character of the studied material. The evolution of the introduced parameter with corresponding the F-D curve of pure copper and Cu-20%SiC composite proceed by SPS and SPS+HPT routine has been shown in fig. 17.

On the one hand, the large deformation brought a significant improvement of pure copper mechanical strength, but on the other did not change considerably the deformation character (fig. 17a and b). At both F-D curves, we can highlight and denote specific stages defining the type of SPT deformation. In the initial stage of loading, the material deforms elastically and the deformation is influenced by Young's modulus and yield strength. In the second stage, an elastoplastic transition occurs and plastic deformation begins to dominate on a much larger sample area. As the deformation covers the entire thickness of the sample range, the third stage begins. Here, it becomes the change in the main deformation mechanism from bending to membrane stretching in the sample. Generally, the moment of the transition is hard to catch on the F-D curve, however it can be exposed by the use of the normalized $\dot{F}$ parameter. In the case of the SPS Cu sample, a vast increase of parameters is seen, which indicates a typical ductile type of deformation. The mentioned feature does not occur in the case of the second sample suggesting a slight transition of deformation type from ductile after SPS to mixed (brittle-ductile) after SPS+HPT (fig. 17b). As it was confirmed by microtensile (fig. 10) and nanoindentation study (fig. 13), HPT reduces significantly the plastic range of deformation of copper in the whole range of the material deformation.

The fourth stage begins with a decrease of $\dot{F}$ parameter which is related to a plastic instability with necking, crack initiation and propagation to failure. At the beginning of the fifth stage, we found macrocracks initiate [25] which is manifested by the descent of the F-D curve - steeper, limited for SPS and flatter, longer for the SPS+HPT sample.

The addition of 20% ceramic SiC reinforcement to the copper matrix, apart from it reduces a tensile strength, remains roughly the character of the F-D curve in comparison to pure SPS copper (fig. 17c). The first stage of deformation reveals an increase of elastic response of composite due to the presence of hard ceramic particles stiffening the entire system. The nearly imperceptible third stage shows the decrease of plastic contribution to deformation defining it as a mixed one (brittle-ductile). The fourth stage is accompanied by crack initiation on the metal-ceramic interface (figs. 9c and e) as the most vulnerable and responsive component of SPS composite to mechanical tension (fig. 10).

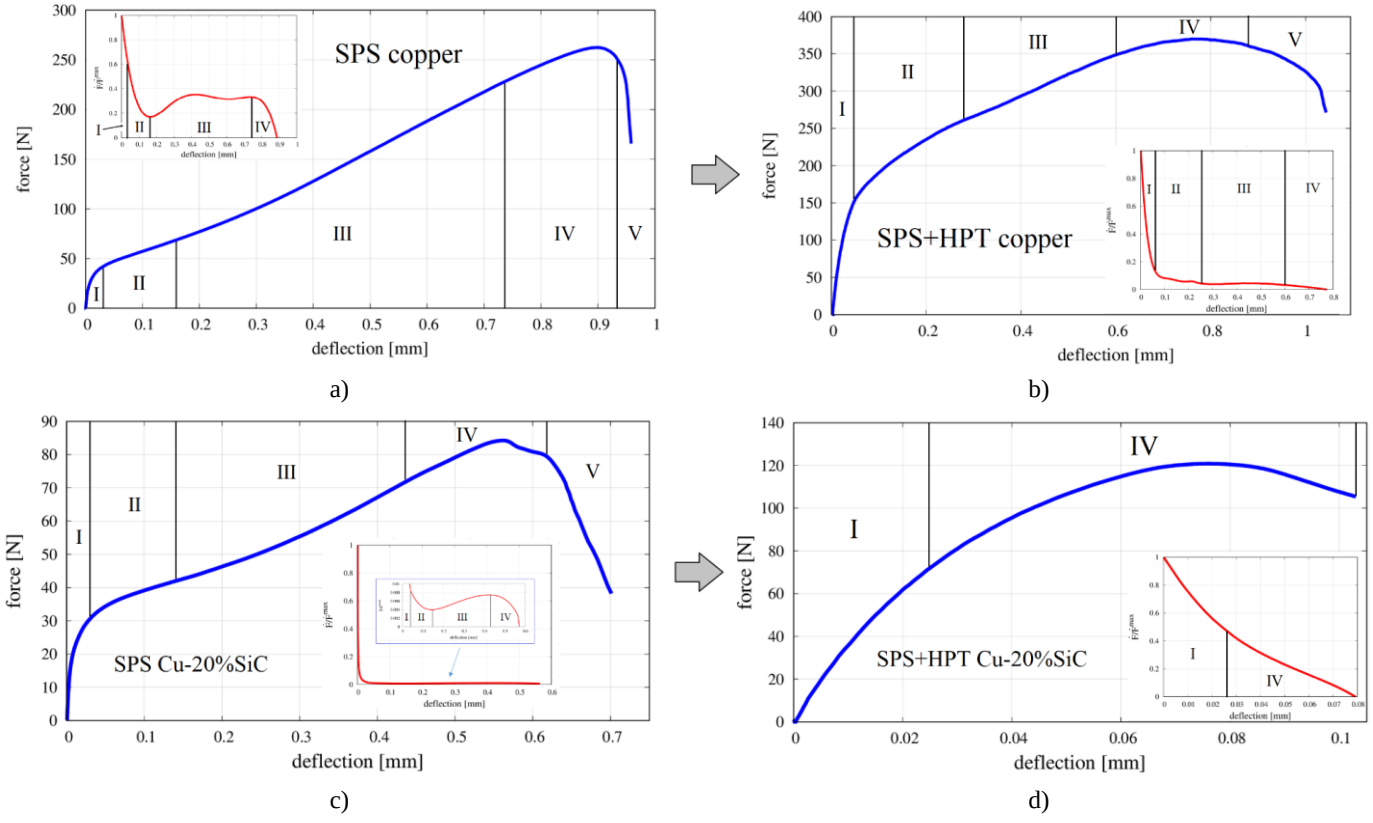

Figure 17. Representative force-deflection curves (with a normalized derivative of force in respect of deflection) of: a) SPS pure copper, b) SPS+HPT pure copper, c) SPS Cu-20%SiC composite and d) SPS+HPT Cu-20%SiC composite.

The higher volumetric content of SiC particles in composite, the more brittleness we may expect. As it was shown in [6], copper matrix composites with 30%, 40% and 50% of ceramic content sintered by SPS breaks in a typical brittle manner. A similar effect can be obtained by the application of large deformation via HPT routine, which switches dramatically the character of deformation and damage manner of composite from mixed (after SPS) to typical brittle one (after HPT) (fig. 17d). In this case, it is possible to distinguish only two stages of deformation - the first one related to elastic response (I stage of SPT deformation) and the second one demonstrating the initiation and propagation of composite damage (IV stage of SPT deformation). Comparing to the SPS composite, I stage of the F-D curve of SPS+HPT composite points out the improved elastic response due to the several strengthening mechanisms of all composite components revealed by micro- and nanolevel investigations. Strengthened copper matrix (induced by grain refinement and lattice defects), the occurrence of nano SiC particles (providing the Orowan effect, the load-bearing effect and load transfer between the matrix and the reinforcement) and interface zone between both phases (supported by an enhanced dislocation density strengthening mechanism) create the beneficial macroscopic system, which ensures the increased composite stiffness.

The transition between I and IV stages of SPT deformation can be identified by the change of curve slope of $\dot{F}$ parameter (fig. 17d). Here, the initial cracking starts transgranular within the partially damaged and weaken SiC particles (figs. 9d and f). As the composite damage propagates, we can expect the further composite components to join the process – intergranular cracking via metal-ceramic interface and copper matrix in a transgranular manner.

5. SUMMARY AND CONCLUSIONS

This research provides a first multiscale investigation of the mechanical properties of pure copper and copper matrix composite reinforced by silicon carbide particles produced by the SPS technique and the combination of SPS and HPT routine. Significant mechanical improvement of SPS+HPT materials has been achieved (comparing to SPS ones) and demonstrated by the performance of small punch (at macroscale), microtensile (at microscale) and nanoindentation tests (at nanoscale). Revealed microstructural and mechanical evolution of each composite component (metal matrix, ceramic reinforcement and metal-ceramic interface) at nano- and microscale has a significant impact on the mechanical response at the macroscopic scale.

An intensified debonding effect of the copper matrix and ceramic reinforcement in SPS samples is due to their relatively low adhesion. This weak bonding is associated with the occurrence of material defects, as well as the formation of Cu_3Si and residual carbon layers caused by the dissolution of silicon into the copper matrix during the powder metallurgy process. As the scanning electron microscopy images of fractured samples reveal, the change in failure mechanism of HPT composites is related to an improvement of the copper-silicon carbide bonding, which exhibits higher strength due to the reduction in defects, the annihilation of Cu_3Si and residual carbon layers and the influence of enhanced dislocation density strengthening acting mainly in the metal-ceramic contact zone. A transition of the dominant failure mechanism for samples processed by HPT is related to the evolution of the structure and the size of the SiC particles. The large and solid particles

prevailing in SPS samples is largely replaced by a high fraction of ceramic nanoparticles. As the ceramic content increases, fragmentation becomes more effective, thereby lowering the numbers of large and damaged particles and raising the numbers of nanoparticles which is reflected in the nanohardness values of the ceramic phase. By applying HPT processing, and thus obtaining a structure with ceramic nanoparticles, the Orowan mechanism becomes responsible for the enhanced strength in the metal matrix relative to pure copper. Likewise, the grain refinement and lattice defects of pure copper samples brought on by HPT strengthen the material keeping ductility at a satisfactory level as the microtensile and nanoindentation results confirmed.

Large deformations applied via HPT processing activates both advantageous and disadvantageous effects influencing the material mechanical behavior during small punch testing. Knowing both the strengthening and weakening impact of HPT on composite properties allows us to characterize the change of deformation and damaged character at the macroscopic level. Micro-grained copper sintered by SPS demonstrates a typical ductile type of deformation and damage with considerable plastic range. HPT processing decreases the plastic component of deformation due to inducing the material's defects and making the deformation type to be a combination of brittle-ductile one. A comparable effect has been observed by the inclusion of ceramic particles within the SPS copper matrix. Finally, the HPT application of composite material impacts mostly the deformation and damage behavior to be a typical representation of the brittle type.

Acknowledgments

These studies were carried out as part of a project financed by the National Science Center within the framework of the OPUS Program (contract ref. no.: 2020/37/B/ST8/03907 and 2014/13/B/ST8/04320). The research was supported by the National Centre for Research and Development (Poland) under grant 246/L-6/14/NCBR/2015 and by the European Research Council under ERC Grant Agreement No. 267464-SPDMETALS.

References

[1] X. Jiang, W. Liu, Y. Li, Z. Shao, Z. Luo, D. Zhu, M. Zhu, Microstructures and mechanical properties of Cu/Ti3SiC2/C/graphene nanocomposites prepared by vacuum hot-pressing sintering and hot isostatic pressing. Compos. B. Eng. 2018;141:203-213.

[2] C. Cai, S. He, L. Li, Q. Teng, B. Song, C. Yan, Q. Wei, Y. Shi, In-situ TiB/Ti-6Al-4V composites with a tailored architecture produced by hot isostatic pressing: Microstructure evolution, enhanced tensile properties and strengthening mechanisms. Compos. B. Eng. 2019;164:546-558.

[3] M. Razavi, A.R. Farajipour, M. Zakeri, M.R. Rahimipour, A.R. Firouzbakht, Production of Al2O3–SiC nano-composites by spark plasma sintering. The Journal of the Spanish Ceramic and Glass Society 2017;56:186-194.

[4] K. Naplocha, Self-propagating high-temperature synthesis (SHS) of intermetallic matrix composites, Intermetallic Matrix Composites, Properties and Applications 2018: 203-220,

[5] P. Bazarnik, S. Nosewicz, B. Romelczyk-Baishya, M. Chmielewski, A. Strojny-Nędza, J. Maj, Y. Huang, M. Lewandowska, T.G. Langdon, Effect of spark plasma sintering and high-pressure torsion on the microstructural and mechanical properties of a Cu–SiC composite, Mater. Sci. Eng. A 2019;766:138350.

[6] S. Nosewicz, B. Romelczyk-Baishya, D. Lumelskyj, M. Chmielewski, P. Bazarnik, D.M. Jarząbek, K. Pietrzak, K. Kaszyca, Z. Pakieła, Experimental and numerical studies of micro- and macromechanical properties of modified copper–silicon carbide composites, Int. J. Solids Struct. 2019;160:187-200.

[7] M. Chmielewski, S. Nosewicz, E. Wyszkowska, Ł. Kurpaska, A. Strojny-Nędza, A. Piątkowska, P. Bazarnik, K. Pietrzak, Analysis of the micromechanical properties of copper-silicon carbide composites using nanoindentation measurements. Ceram. Int. 2019;45(7A):9164-9173.
[8] A.R. Zurnachyan, S.L. Kharatyan, H.L. Khachatryan, A.G. Kirakosyan, Self-propagating high temperature synthesis of SiC–Cu and SiC–Al cermets: role of chemical activation. Int. J. Refract. Metals. Hard. Mater. 2011;29:250–255.
[9] I. Sabirov, O. Kolednik, R. Pippan, Homogenization of metal matrix composites by high-pressure torsion. Metall. Mat. Trans. A 2005;36:2861.
[10] M. Ebrahimi, M.H. Shaeri, C. Gode, H. Armoon, M. Shamsborhan, The synergistic effect of dilute alloying and nanostructuring of copper on the improvement of mechanical and tribological response. Compos. B. Eng. 2019;164:508-516.
[11] L. Xiong, J. Shuai, K. Liu, Z. Hou, L. Zhu, W. Li, Enhanced mechanical and electrical properties of super-aligned carbon nanotubes reinforced copper by severe plastic deformation. Compos. B. Eng. 2019;160:315-320.
[12] F. Ferreira, I. Ferreira, E. Camacho, F. Lopes, A.C. Marques, A. Velhinho, Graphene oxide-reinforced aluminium-matrix nanostructured composites fabricated by accumulative roll bonding. Compos. B. Eng. 2019;164:265-271.
[13] J.K. Han, X. Li, R. Dippenaar, K.D. Liss, M. Kawasaki, Microscopic plastic response in a bulk nano-structured TiAl intermetallic compound processed by high-pressure torsion. Mater. Sci. Eng. A 2018;714:84-92.
[14] P. Bazarnik, B. Romelczyk, Y. Huang, M. Lewandowska, T.G. Langdon, Effect of applied pressure on microstructure development and homogeneity in an aluminium alloy processed by high-pressure torsion. J. Alloy. Compd. 2016;688:736–745.
[15] P. Bazarnik, Y. Huang, M. Lewandowska, T.G. Langdon,. Structural impact on the Hall–Petch relationship in an Al–5Mg alloy processed by high-pressure torsion. Mater. Sci. Eng. A 2015;626:9-15.
[16] V.V. Stolyarov, Y.T. Zhu, T.C. Lowe, R.K. Islamgaliev, R.Z. Valiev, Processing nanocrystalline Ti and its nanocomposites from micrometer-sized Ti powder using high pressure torsion, Mater. Sci. Eng. A 2000;282:78-85.
[17] M.M. de Castro, A.P. Carvalho, P.H.R. Pereira, A.C. Isaac Neta, R.B. Figueiredo, T.G. Langdon, Consolidation of magnesium and magnesium alloy machine chips using high-pressure torsion. Mater. Sci. Forum 2018;941:851-856.
[18] B. Ahn, A.P. Zhilyaev, H.J. Lee, M. Kawasaki, T.G. Langdon, Rapid synthesis of an extra hard metal matrix nanocomposite at ambient temperature. Mater. Sci. Eng. A 2015;635:109-117
[19] L. Ceschini, A. Dahle, M. Gupta, A.E.W. Jarfors, S. Jayalakshmi, A. Morri, F. Rotundo, S. Toschi, A.W. Singh, Metal Matrix Nanocomposites: An Overview. Springer, Singapore, 2017.
[20] M. Chmielewski, K. Pietrzak, M. Teodorczyk, S. Nosewicz, D.M. Jarzabek, R. Zybała, P. Bazarnik, M. Lewandowska, A. Strojny-Nedza, Effect of metallic coating on the properties of copper-silicon carbide composites. Appl. Surf. Sci. 2017;421A:159-169.
[21] M. Chmielewski, K. Pietrzak, A. Strojny-Nędza, K. Kaszyca, R. Zybala, P. Bazarnik, M. Lewandowska, S. Nosewicz, Microstructure and thermal properties of Cu-SiC composite materials depending on the sintering technique. Sci. Sinter. 2017;49:11-22.
[22] M.I.A. el Aal, Effect of high-pressure torsion processing on the microstructure evolution and mechanical properties of consolidated micro size Cu and Cu-SiC powders. Adv. Powder Technol. 2017;28:2135–2150.
[23] M. Jahedi, M.H. Paydar, M. Knezevic, Enhanced microstructural homogeneity in metal-matrix composites developed under high-pressure-double-torsion. Mater. Charact. 2015;104:92-100.
[24] C. Rodríguez, M. Fernández, J.G. Cabezas, T.E. García, F.J. Belzunce, The use of the small punch test to solve practical engineering problems, Theoretical and Applied Fracture Mechanics, 2016;86:109-116.
[25] S. Rasche, M. Kuna, Improved small punch testing and parameter identification of ductile to brittle materials, International Journal of Pressure Vessels and Piping, 2015;125:23-34.
[26] D.M. Jarząbek, M. Chmielewski, T. Wojciechowski, The measurement of the adhesion force between ceramic particles and metal matrix in ceramic reinforced-metal matrix composites, Composites Part A: Applied Science and Manufacturing 2015;76:124-130.
[27] C. Oliver, G.M. Pharr, An improved technique for determining hardness and elastic modulus using load and displacement sensing indentation. J. Mater. Res. 1992;7:1564–1583.
[28] T. Schöberl, I. Sabirov, R. Pippan, Nanoindentation applied on a tungsten–copper composite before and after high-pressure torsion. Inter. J. Mater. Res. 2005;96(9):1056–1062.
[29] Z. Zhang, D.L. Chen, Consideration of Orowan strengthening effect in particulate-reinforced metal matrix nanocomposites: a model for predicting their yield strength. Scripta Mater 2006;54:1321-1326.

[30] Y.Z. Tian, J.J. Li, P. Zhang, S.D. Wu, Z.F. Zhang, M. Kawasaki, T.G. Langdon, Microstructures, strengthening mechanisms and fracture behavior of Cu-Ag alloys processed by high-pressure torsion, Acta Mater. 2012;60:269-281.
[31] J. Čížek, M. Janeček, O. Srba, R. Kužel, Z. Barnovská, I. Procházka, S. Dobatkin,Evolution of defects in copper deformed by high-pressure torsion, Acta Materialia, 2011;59(6): 2322-2329,
[32] Valiev, Ruslan & Islamgaliev, Rinat & Alexandrov, I.V. Bulk Nanostructured Materials from Severe Plastic Deformation. Progress in materials science, 2000;45:103-189.
[33] R. Casati, M. Vedani, Metal Matrix Composites Reinforced by Nano-Particles—A Review. Metals 2014;4:65-83.
[34] D. Hull, D.J. Bacon, Introduction to Dislocations, 4th ed.; Butterworth Einemann: Oxford, UK, 2001.
[35] F.A. Mirza, D.L. Chen, A Unified Model for the Prediction of Yield Strength in Particulate-Reinforced Metal Matrix Nanocomposites. Materials 2015;8:5138-5153.
[36] H. Zhang, N. Maljkovic, B.S. Mitchell, Structure and interfacial properties of nanocrystalline aluminum/mullite composites. Mater. Sci. Eng. A 2002;326:317–323.
[37] K.K. Chawla, Interfaces in metal matrix composites. Compos. Interface. 2012;4(5):287-298.
[38] X. Zhang, B. Zhang, Y. Mu, S. Shao, C.D. Wick, B.R. Ramachandran, W.J. Meng, Mechanical failure of metal/ceramic interfacial regions under shear loading. Acta Mater. 2017;138:224-236.
[39] L. Li, Z. Xia, Role of interfaces in mechanical properties of ceramic matrix composites, Advances in Ceramic Matrix Composites, 2018:355–374.
[40] M.R. Akbarpour, S. Alipour, Wear and friction properties of spark plasma sintered SiC/Cu nanocomposites. Ceram. Int. 2017;43(16):13364-13370.
[41] L. Zhang, X. Qu, B. Duan, X. He, M. Qin, S. Ren, Wettability and pressureless infiltration mechanism in SiC-Cu systems. Int. J. Miner. Metal. Mater. 2009;16(3):327-333.
[42] H.K. Kang, S.B. Kang, Thermal decomposition of silicon carbide in a plasma-sprayed Cu/SiC composite deposit. Mater. Sci. Eng. A 2006;428:336-345.
[43] R.R. Chromik, W.K. Neils, E.J. Cotts, Thermodynamic and kinetic study of solid state reactions in the Cu–Si system. J. Appl. Phys. 1999;86:4273-4281.
[44] K. Suganuma, K. Nogi, Interface Structure Formed by Characteristic Reaction between α-SiC Single Crystal and Liquid Cu. J Jpn. I Met. 1995;59:1292-1298.
[45] C. Goh, J. Wei, L. Lee, M. Gupta, Properties and Deformation Behavior of Mg-Y2O3 Nanocomposites. Acta Mater. 2007:55:5115-5121.
[46] A. Sanaty-Zadeh, Comparison between current models for the strength of particulate-reinforced metal matrix nanocomposites with emphasis on consideration of Hall-Petch effect. Mater. Sci. Eng. A 2012;531:112–118.
[47] R.U. Vaidya, K.K. Chawla, Thermal expansion of metal-matrix composites. Compos Sci Technol 1994;50:13-22.
[48] S.M. Choi, H. Awaji, Nanocomposites - A New Material Design Concept, Sci. Technol. Adv. Mat. 2005;6(1):2-10.
[49] D.C. Dunand, A. Mortensen, Reinforced Silver Chloride as a Model Material for the study of Dislocations in Metal Matrix Composites. Mater. Sci. Eng. A 1991;144:179-188.
[50] R.J. Arsenault, N. Shi, Dislocation generation due to differences between the coefficients of thermal expansion, Mater. Sci. Eng. 1986;81:175-187.